Available online at www.sciencedirect.com
ScienceDirect
Trans. Nonferrous Met. Soc. China 27(2017) 2282−2290
Transactions of Nonferrous Metals Society of China
www.tnmsc.cn

Evaluation of flow behavior in copper electro-refining cell with different inlet arrangements

Ping ZHOU[1], Hai-bo MA[1], Zi-wei XIE[1], Hong-jie YAN[1], Chenn Q. ZHOU[1,2]

1. School of Energy Science and Engineering, Central South University, Changsha 410083, China;
2. Center for Innovation through Visualization and Simulation, Purdue University Northwest, 2200 169th Street, Hammond, IN 46323, USA

Received 20 May 2016; accepted 15 December 2016

Abstract: The arrangement of electrolyte inlet in the copper electro-refining (ER) cell has a great influence on the local flow field, which affects the distribution of electrical current density in consequence. In order to understand the complicated phenomena of electrolyte flow behavior in vertical counter electrodes in full-scale copper ER cell, the three-dimensional computational fluid dynamics (CFD) models with four different arrangements of electrolyte inlets, i.e., single inlet (SI), central bottom inlets (CBI), top side interlaced inlets (TII), and bottom side interlaced inlets (BII), were established to simulate the flow behavior. Simulation results have revealed that the parallel injection devices help to improve the electrolyte velocity between electrodes, and while the relative range of electrolyte velocity in CBI exceeds that of TII and BII, which is more than 4 times, indicating its severer unequal flow distribution. Meanwhile, the average velocity of electrolyte in BII is 4 times larger than that of SI due to its higher turbulence intensity. Generally, one of the efficient ways to supply fresh copper solution rapidly and uniformly into the inter-electrode space is to adapt the arrangement of BII. By utilizing such an arrangement, the electro-refining under high electrical current density is possible, and the productivity can be increased in sequence.

Key words: copper electro-refining; electrolyte inlet arrangement; flow uniformity; computational fluid dynamics

1 Introduction

Copper electro-refining (ER) is an essential process widely used in industry to produce high purity copper. The traditional industrial copper electro-refining process has been operated in several hundreds of cells with dozens of anodes and cathodes aligned alternately in electrolyte. Copper is dissolved from the anode plate into the electrolyte and deposits onto the opposing cathode by means of the passage of electrical current between the electrode plates. The main purpose is not only to obtain pure copper but also to separate valuable impurities (i.e., gold and silver) from the anodes. As is well known, one of the most efficient ways to improve productivity is to increase the electrical current density [1]. But in traditional ER cell with the arrangement of single inlet (SI), the natural convection, which is driven by cupric ion concentration gradients between boundary layer and the bulk-electrolyte, governs the flow patterns along vertical electrodes [2,3], leading to insufficient circulation of electrolyte flow between electrodes. In this situation, the electrolyte flows upward on the cathode surface and downward on the anode surface, and copper cannot be supplied to the cathode surface at the rate depleted from the boundary layer by plating [4,5]. As a result, the traditional ER cell with the arrangement of SI operates at a limited electrical current density, normally 220−280 A/m^2, and it is not helpful to control the concentration polarization along a tall electrode under a high electrical current density [6].

Therefore, the idea of copper ER cell with parallel injection devices was put forward by METTOP, known as the METTOP-BRX-Technology [7]. In this type of ER cell, dozens or even hundreds of jet orifices are installed either on the side walls or beneath the bottom of cathodes rather than located at one end. Thus, the electrolyte can directly enter the gap between each pair of electrode plates, and then overflow through the outlet located at one end of the cell. In this way, sufficient fresh electrolyte can be provided to the boundary layer in the vicinity of the electrode surface where copper is

Foundation item: Project (61321003) supported by the National Natural Science Foundation of China
Corresponding author: Chenn Q. ZHOU; Tel: +1-219-989-2665; E-mail: czhou@pnw.edu
DOI: 10.1016/S1003-6326(17)60254-1

depleted. As a result, electro-refining under high electrical current density is possible.

As the quantity and location of injection devices have significant effects on the local flow patterns, and consequently, the distribution of electrical current density and cupric ion deposition, it is necessary to understand the flow field between electrode plates and the differences in the arrangements of electrolyte inlets [8]. However, though a great deal of theoretical and experimental work has been devoted to the velocity of electrolyte and concentration profiles of natural convection in the traditional copper ER cell [9−11], only a limited number of computational fluid dynamics (CFD) modeling studies in a full scale copper ER cell with parallel injection devices have taken place [12], and indeed, very few have compared the difference among different arrangements of electrolyte inlets comprehensively.

It is intended in the present work to numerically analyze the electrolyte flow field in the three-dimensional full-scale copper ER cell with four different arrangements of electrolyte inlets. By evaluating both electrolyte flow behavior and the updating speed of fresh copper electrolyte, the results are expected to be useful for the design of copper ER cell in the future.

2 Model description

2.1 Structure of copper ER cell

The physical model of the copper ER cell applied in the present study is 5.84 m in length, 1.17 m in width and 1.4 m in depth. 55 anodes with 1 m in height and 0.965 m in width and 54 cathodes with 1.035 m in height and 1.01 m in width are alternately arranged. The thicknesses of anode and cathode are 10 mm and 3.25 mm, respectively. The distance between the centers of every two anodes (or cathodes) is fixed to be 100 mm. As indicated previously, four different arrangements of electrolyte inlets are modeled as follows.

1) SI (Single inlet) arrangement. In this situation, electrolyte is charged from a single inlet of 50 mm in diameter, which is located at one end of the cell, as shown in Fig. 1. This kind of arrangement has been adopted worldwide in the past few decades.

2) CBI (Central bottom inlet) arrangement. The electrolyte is introduced to the cell through a single supply pipe, which is 100 mm below the bottom of cathodes and extends along the whole cell. Meanwhile, 62 jet orifices of two different sizes are placed in three separate locations (i.e., locations A, B and C) on the supply pipe, as shown in Fig. 2.

Specifically, 20 jet orifices of 6 mm in diameter are located between the first and the last five electrode pairs marked as A and C in Fig. 2(b). Thus, each electrode pair

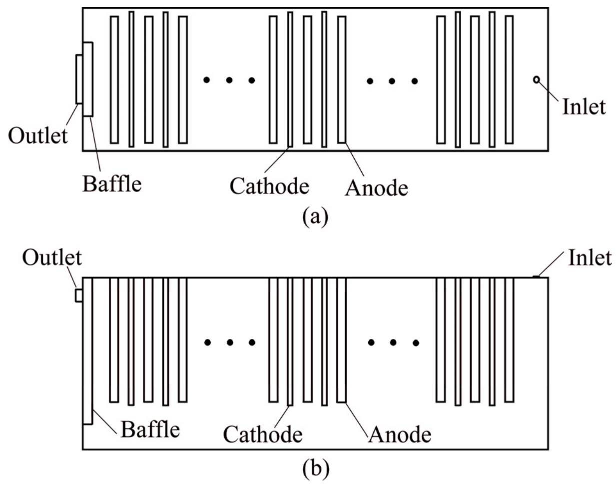

Fig. 1 Schematic diagrams of SI arrangement: (a) Top view; (b) Side view

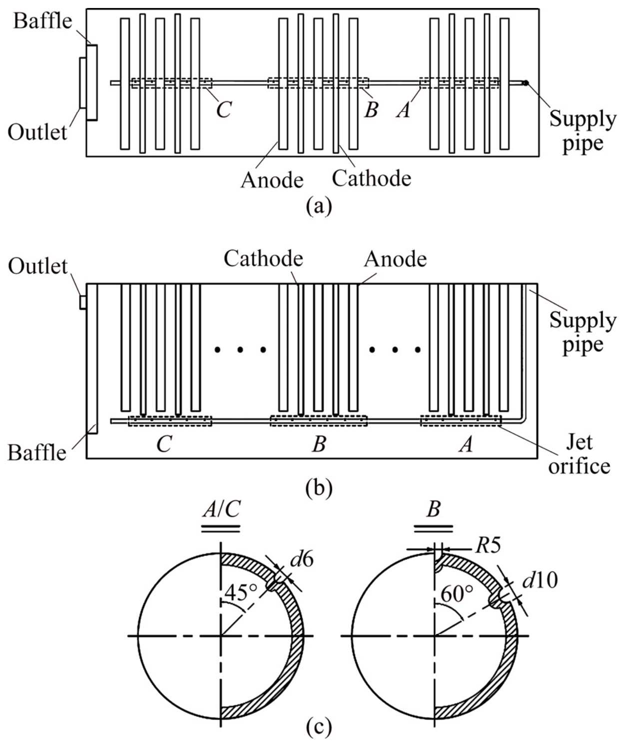

Fig. 2 Schematic diagrams of CBI arrangement: (a) Top view; (b) Side view; (c) Cross sections of jet orifices

can be fed by two jet orifices, which are rotated 45° clockwise and counterclockwise from the vertical plane, as shown in Fig. 2(c). While another 42 jet orifices of 10 mm in diameter are placed between 14 electrode pairs in the middle of the cell, which are marked as B in Fig. 2(b). For those 14 electrode pairs, there are 3 jet orifices that can supply fresh electrolyte for each pair, and two of them are rotated 60° clockwise and counterclockwise from the vertical plane, respectively, as shown in Fig. 2(c).

3) TII (Top side interlaced inlet) arrangement. The

electrolyte is horizontally fed to the gaps between each pair of electrodes by 108 interlaced jet orifices of 4 mm in diameter placed on both supply pipes, which are installed on both side walls of the copper ER cell and are 50 mm lower than the top of the cathodes, as well as the free surface of electrolyte as shown in Fig. 3. In other words, one jet orifice is assigned to each pair of electrodes to provide electrolyte during the electrolysis process.

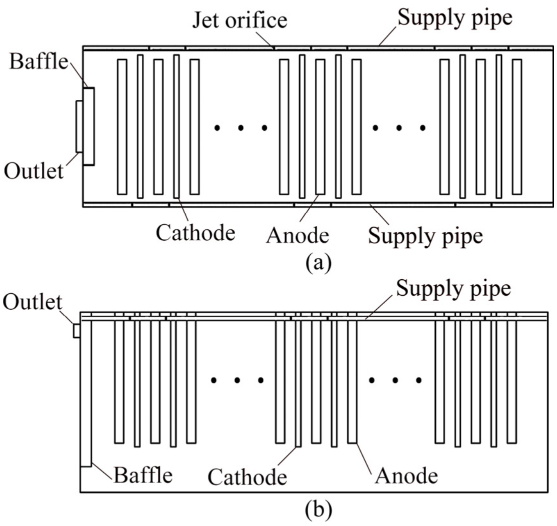

Fig. 3 Schematic diagrams of TII arrangement: (a) Top view; (b) Side view

4) BII (Bottom side interlaced inlet) arrangement. Contrary to the arrangement of TII, the two supply pipes with 108 jet orifices are placed 100 mm below the lower end of the cathodes, as shown in Fig. 4. And the jet orifices are set in the same way as the arrangement of TII.

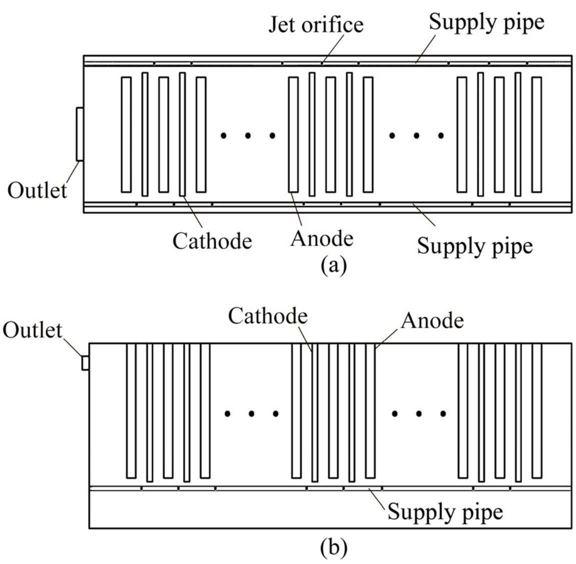

Fig. 4 Schematic diagrams of BII arrangement: (a) Top view; (b) Side view

The outlets in the four cases are all placed at the downstream end of the cell. In order to prevent the electrolyte flowing directly to the outlet, a steel baffle is installed between outlet and the last electrode plate in the cases of SI, CBI, and TII. However, its influence on the flow field is negligible [13].

2.2 Mathematical models

To simulate the electrolyte flow in copper ER cell, the following assumptions are made.

1) The electrolyte is assumed to be incompressible Newtonian fluid.

2) The electrolysis process is in the steady state.

3) The surface of electrolyte is assumed to be free surface.

4) The sedimentation of anode slime and rise of anode bubble are neglected. Therefore, the multi-phase flow is simplified to a single-phase flow.

As indicated by LEAHY and SCHWARZ [2], the electrolyte flow is not suitable to be considered as laminar if the gap between electrodes exceeds 24 mm, which corresponds to a Reynolds number of 256. However, this type of turbulence is different from the traditional shear-driven turbulence, but rather comes from a delicate near-wall instability caused by the interaction between copper concentration and flow. In the present study, the Reynolds numbers for SI, CBI, TII and BII are 549, 783, 852 and 912, respectively. Therefore, the physical laws applied in this study are Navier−Stokes equations and the kinetic energy (k)−eddy frequency (ω) shear-stress-transport (SST) turbulence model, due to its improved velocity profile prediction close to the wall and modifications for low Reynolds number flow [2]. The k−ω SST model effectively blends the robust and accurate formulation of the k−ω model in the near-wall region with the free-stream independence of the k−ε model in the far field by introducing a blending function. The turbulent viscosity can be written in terms of kinetic energy k and eddy frequency ω as follows [14]:

$$\mu_{\mathrm{T}}=\frac{a_1 k}{\max(a_1\omega, SF_2)} \tag{1}$$

where F_2 is a blending function that is designed to be one in the near-wall region, which activates the standard k−ω model, and zero away from the surface, which activates the k−ε model. S is the strain rate magnitude, and α_1 is a dimensionless parameter, which is set to be 5/9.

2.3 Operating conditions

The detailed physical properties of electrolyte and operating conditions of ER cell are listed in Table 1.

According to DENPO et al [6], the mesh size in the vicinity of the electrode surface and the gap between electrode plates should be as fine as possible to identify the turbulence. On the other hand, the CPU time and technology of computers today have to be taken into consideration. Thus, the mesh size of the first cell in front of the electrodes is set to be 0.08 mm, and there are at least 20 meshes in the inter-electrode space based on Kawai's work [8]. Therefore, the total computational meshes of about 7×10^6 with average mesh skewness of 0.26 and aspect ratio of 1.96 are adopted for each case in the following study. No slip boundary condition is applied at both bottom and side walls. Also, the zero flux boundary condition is set at all the walls. All of the cases are developed based on the platform of the software package ANSYS-Fluent 15.0.

Table 1 Physical properties of electrolyte and operating conditions of ER cell

Parameter	Value
Flow rate/($L\cdot min^{-1}$)	35
Electrolyte density/($kg\cdot m^{-3}$)	1211.9
Electrolyte viscosity/($Pa\cdot s$)	1.02×10^{-3}

3 Results and discussion

3.1 Electrolyte flow patterns

Figure 5 shows the velocity contours of electrolyte in the vertical middle section of the cell, and the diagrams are colored by the magnitude of the flow velocity. In the arrangement of SI, the electrolyte is fed from a single inlet, thus, a high velocity area near the inlet can be observed in Fig. 5(a). After reaching the bottom of the cell, the electrolyte flows toward the outlet located at the opposite end through the bulk region below the lower end of electrodes. Meanwhile, a small portion of the electrolyte flows upward and then enters the interspaces between electrode pairs. However, this phenomenon mostly occurs in just a few pairs close to the inlet, while the electrolyte in other electrode pairs can hardly be updated. As a result, the flow velocities in most of the electrode pairs are relatively slow, which means that fresh copper electrolyte may not be supplied in time during the electro-refining process.

In the arrangement of CBI, the electrolyte is introduced to the cell through multiple injection devices from three different locations under the bottom of electrodes. At such locations, the electrolyte is injected directly into the inter-electrode spaces, and then moves upward till gravity and viscosity force hinder this movement, as shown in Fig. 5(b). In this kind of arrangement, the electrolyte between many electrode pairs can be circulated by the injection due to the increase in the number of inlets compared with that of SI. However, the velocities of electrolyte in the inter-electrode spaces between injection locations are still relatively low.

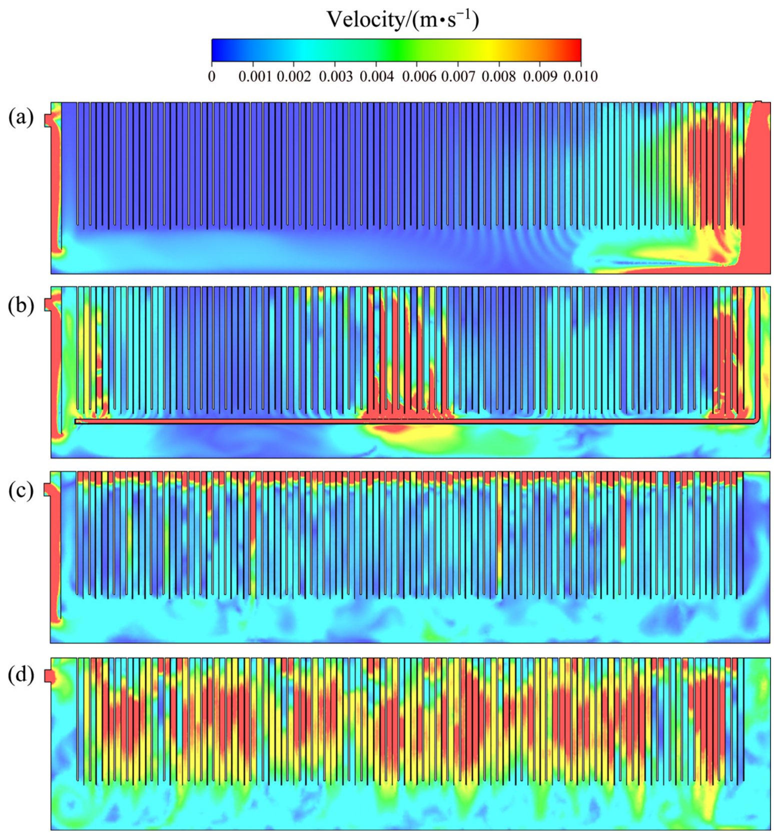

Fig. 5 Velocity contours of electrolyte on vertical middle section: (a) SI; (b) CBI; (c) TII; (d) BII

In the arrangement of TII, the electrolyte is supplied horizontally to each electrode pair from supply pipes placed at the top of side walls. It then flows downward along the vertical electrode plates and finally joins the main stream in the bottom bulk region, which is shown in Fig. 5(c). Contrary to the arrangement of SI and CBI, the distribution of electrolyte flow in this kind of arrangement is much more uniform, which can be attributed to the equally spaced inlets. Similar to arrangement of TII, the electrolyte also enters each electrode pair by alternatively arranged injection devices in the arrangement of BII, but the flow is injected vertically from the supply pipes under the bottom of the electrodes. Thus, the distribution of electrolyte flow in the whole cell is as uniform as that of TII, as shown in Fig. 5(d).

In order to comprehensively understand the flow patterns in the inter-electrode spaces, three vertical central planes in the interspaces of the 5th, 55th, and 105th electrode pairs are selected as monitor planes.

Figure 6 illustrates the velocity profiles of electrolyte in the 5th, 55th, and 105th monitor planes. The velocity distribution of electrolyte shows that the flow patterns in the inter-electrode spaces are determined by the ways of inlet arrangements. It can be found from Fig. 6(a) that in the arrangement of SI, the fresh electrolyte enters inter-electrode spaces from the upper side regions of the cell successively, and it is then drawn down into the bottom region underneath the electrodes by gravity. Furthermore, a few eddies are observed in the 5th plane due to the higher flow velocity near the inlet, whereas the flow fields in the 55th and 105th planes far away from the inlet are relatively quiescent and uniform.

On the contrary, in the arrangement of CBI, the electrolyte is injected from the bottom of electrodes, then it moves upward and splits into two streams at the top of the interspace. Thus, two symmetric loops circulating in opposite directions can be seen in Fig. 6(b) evidently. In the arrangement of TII, the forced convection caused by free jets has significant influences in the regulation of flow fields corresponding to Fig. 6(c). As blocked by the opposite side wall of the cell, the electrolyte injected horizontally flows downward and reenters the inter-electrode space from the bottom region under the electrodes. As to the arrangement of BII, the vertically injected electrolyte moves upward clinging to the side wall, and it falls into the inter-electrode space after reaches the upper part of the electrodes.

In addition, it is worth noticing that two free jets occur in every inter-electrode space as if there were two inlets placed symmetrically in each pair of electrodes, as shown in Fig. 6(d). A possible reason to explain this is that the flow fed from alternatively arranged injection devices will enter more than one pair of electrodes, as shown in Fig. 7, thus there are two streams in each pair of electrodes: the mainstream injected from the injection

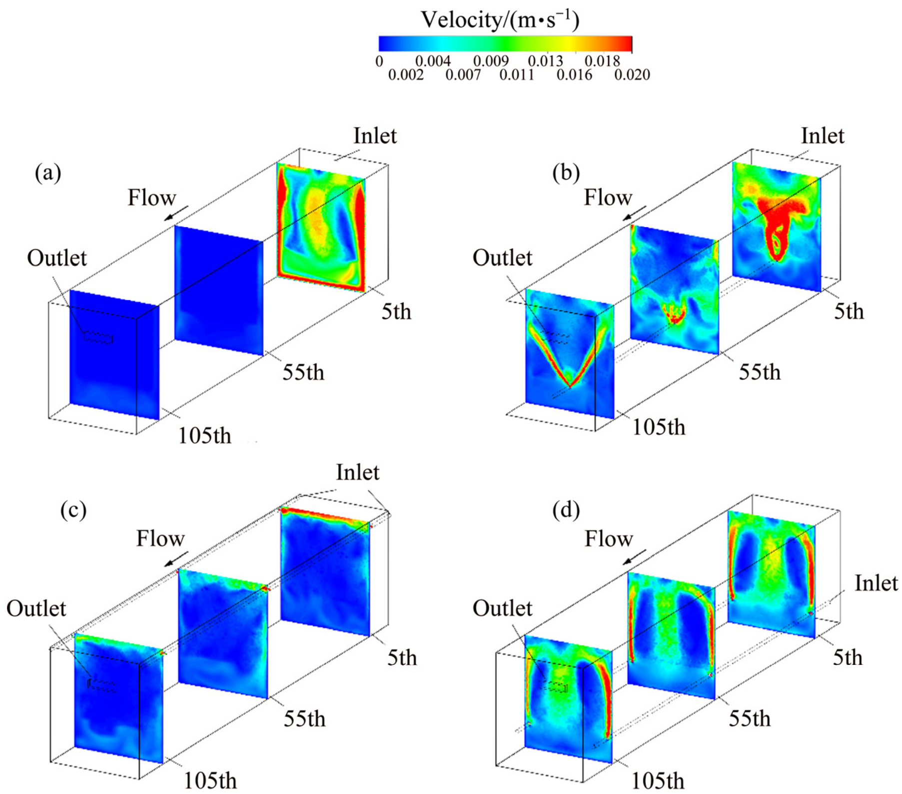

Fig. 6 Velocity contours of electrolyte in the 5th, 55th and 105th electrode pairs: (a) SI; (b) CBI; (c) TII; (d) BII

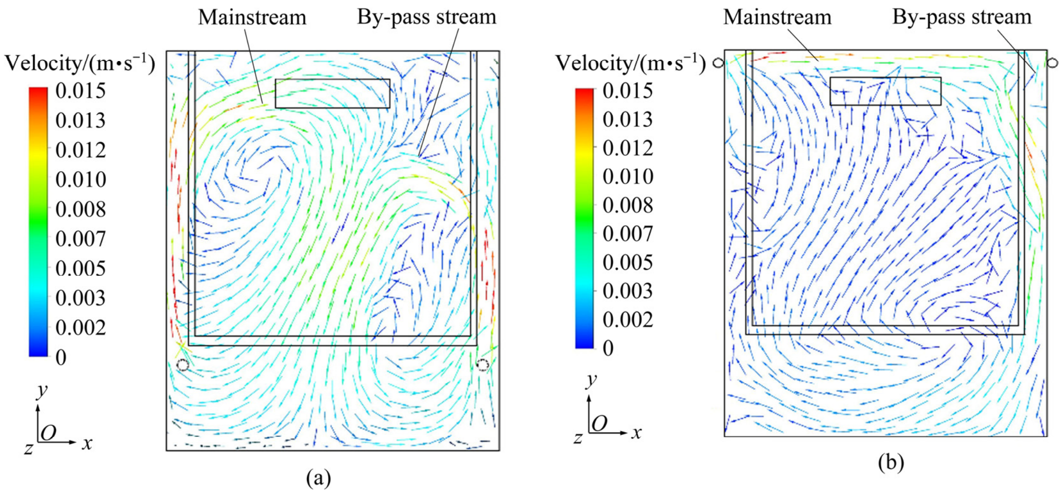

Fig. 7 Schematic diagrams of local flow field in interspaces with different arrangements: (a) BII; (b) TII

device located between this particular electrodes pair and the by-pass stream from the surrounding electrodes pairs. Hence, the distribution of local flow field in the interspaces depends on the interactions between the mainstream and the by-pass stream. In the arrangement of TII, the by-pass stream encounters with the mainstream in the opposite direction while the mainstream has not fully developed. As a result, the by-pass stream counteracts the momentum of the mainstream to some extent. For the arrangement of BII, there is enough space for the mainstream to develop without any blockage, and the two streams in the same direction merge together in the middle of the cell. Therefore, two circulation loops are formed, which results in a more turbulent flow field in the interspaces.

3.2 Flow velocity and uniformity of electrolyte between electrodes

For quantitatively analyzing flow patterns in different arrangements, the volume-weighted average velocity (VWAV) $\bar{u}$ is employed. The volume-weighted average velocity indicates "how fast" the electrolyte circulates in the control volume within the inter-electrode space between each electrode pair, and it can be defined as

$$\bar{u}=\frac{1}{V}\int u\mathrm{d}v=\frac{1}{V}\sum_{i=1}^{n}|u_i|V_i \tag{2}$$

where u expresses electrolyte velocity, V is the control volume, subscribe i refers to number of the ith grid, and n is the number of grids in the region of interest.

Table 2 shows the maximum and minimum values of VWAV in the interspaces between each electrode pair, together with the average value of the entire ER cell in each arrangement. This indicates that the values of VWAV are sensitive to the arrangement of inlets. Obviously, the peaks of VWAV correspond to the locations where electrolyte is fed, especially in the situations of SI and CBI, which can be easily understood on the basis of Eq. (2) and Fig. 5. Compared with the arrangements of TII and BII, SI and CBI will introduce a non-uniform distribution of flow field in the cell, while the application of equally spaced inlets, i.e., TII and BII, makes significant contributions to the distribution of flow field in the cell.

Table 2 Comparison of maximum, minimum and average VWAV values of four cases

Inlet arrangement	VWAV/(10^3m·s^{-1})		
	Inter-electrode space between each pair		Entire ER cell
	Minimum	Maximum	
SI	0.015	9.38	1.28
CBI	0.329	16.252	2.747
TII	1.152	4.8	3.005
BII	1.422	6.799	5.157

Obviously, the arrangement of BII exceeds the other three in terms of average value of VWAV of entire ER cell, which is over four times than that of SI. This phenomenon can be explained by Fig. 6(d) that free jets from different inlets in an adjacent area interfere with each other, which intensifies flow turbulence. It is also can be seen that the maximum value of VWAV in the arrangement of CBI is much greater than that of any other arrangement, mainly due to the higher flow rate through each inlet.

In order to evaluate the flow distribution and uniformity in the inter-electrode spaces, two important flow distribution factors β (in terms of standard deviation) and ξ (in terms of relative range) have been adopted in the present study and can be computed by the following definitions [15]:

$$\beta = \frac{1}{\bar{u}}\sqrt{\frac{1}{n}\sum_{i=1}^{n}(u_i - \bar{u})^2} \times 100\% \tag{3}$$

$$\xi = \frac{1}{\bar{u}}(u_{\max} - u_{\min}) \tag{4}$$

where $u_{\max}$ and $u_{\min}$ refer to the maximum and minimum values of VWAV in the interspaces between each electrode pair, respectively.

The flow distribution uniformity factors β and ξ for all of the cases are shown in Table 3. According to the definitions shown in Eqs. (3) and (4), the factor β indicates the difference between the maximum velocity and the average velocity, while the factor ξ expresses the difference between the maximum velocity and the minimum velocity. As shown in Table 3, the value of standard deviation β decreases with the application of parallel injection devices, which reflects a more uniform flow distribution in the inter-electrode spaces in such an ER cell with parallel injection devices. Moreover, the standard deviation β in the arrangement of BII is 48% less than that of TII, suggesting a less uniform flow distribution in the arrangement of TII. One of the possible reasons can be contributed to the interactions between the main stream and the by-pass stream, as shown in Fig. 7. In the arrangement of TII, the main stream and the by-pass stream enter the inter-electrode space in an opposite direction, which could cause a severe fluctuation of flow between two electrodes. However, in the arrangement of BII, the main stream and the by-pass stream fall together in the same direction, which helps increase electrolyte velocity without bringing any intense fluctuation.

As for the relative range ξ, it maintains a relatively small value in the arrangements of TII and BII shown in Table 4. As mentioned previously, there are three different electrolyte injection positions located in the ER cell in the arrangement of CBI, and only the electrodes within the injection area can be fed with electrolyte by injection devices, as shown in Fig. 2, while the rest of the electrodes mainly depend on the bulk motion of flow to obtain fresh electrolyte for continuous electro-refining. In fact, this kind of arrangement can be considered as partly parallel injection, which is a transition form from the traditional cell to the parallel injection cell. As a result, the velocity of electrolyte flow within the injection area exceeds that in the area without any direct supplement device, causing a much more significant difference between the maximum and minimum velocity. On the contrary, in the cases with equally spaced parallel injection devices, the relative percent range ξ is 90% less than that of CBI, which is almost independent of the installation of parallel injection devices: either near the top of the ER cell or beneath the bottom of the cathodes. In general, the parallel injection devices have the advantage of uniformly distributed electrolyte flow into the inter-electrode spaces, which guarantee the generation of a smooth metal surface on the cathodes.

Table 3 Comparison of flow distribution uniformity factors of four cases

Inlet arrangement	Standard deviation, β/%	Relative range, ξ
SI	0.115	7.316
CBI	0.093	5.797
TII	0.089	1.214
BII	0.046	1.043

Table 4 Comparison of turbulent intensity in four cases

Inlet arrangement	Average of turbulent intensity/%	Standard deviation/%	Relative range
SI	3.254	5.915	8.058
CBI	3.281	3.943	6.032
TII	3.391	0.709	1.142
BII	5.947	0.729	0.77

3.3 Turbulence intensity of electrolyte between electrodes

As pointed out by many researchers [6,16], turbulent mass transfer has considerable influences on the local concentration distribution. On the other hand, a high forced convection increases the diffusion of copper ions by making them transfer faster through eddy flux [17]. The turbulent intensity (I) can be defined as follows [2]:

$$I = \frac{u'}{\bar{u}} \times 100\% \tag{5}$$

where u' is the root-mean-square of the turbulent velocity fluctuations, and $\bar{u}$ is the mean flow velocity.

As shown in Eq. (5), the value of turbulence intensity directly represents the strength of the turbulence in the flow. Table 4 lists the average value of turbulence intensity for the entire ER cell in each arrangement, as well as its standard deviation and relative range. It is obvious that intense turbulent flow can be observed in the region close to the inlets regardless of their arrangements. The reason is that the momentum of injected electrolyte is reduced along the ER cell due to the resistance of viscosity. As shown in Table 4, the standard deviation and relative range of turbulent intensity of the electrolyte in the ER cells with the arrangements of SI and CBI are several times larger than that of the other two arrangements. While the average turbulent intensities of electrolyte in the ER cell with both arrangements of TII and BII exceed those of SI and CBI. This reflects that turbulence is non-uniformly introduced into the inter-electrode space in the arrangements of SI and CBI, resulting in insufficient mass transfer of copper ions. One solution to overcome this deficiency is to install parallel injection devices all over the ER cell, which have the ability to introduce turbulence in the inter-electrode space and promote the convection of electrolyte consequently.

In general, the way that the injected electrolyte circulates in the inter-electrode space is also important to the distribution of turbulence. As shown in Fig. 6, a less turbulent region exists in the center of the electrolyte circulation loop between electrode pair, which associates with relative low velocity where fresh electrolyte is insufficiently supplied. With the aid of the by-pass flow, this region can be minimized to some extent in the arrangement of BII compared with that of TII. This phenomenon can be contributed to the much more turbulent flow field caused by injection devices placed under the bottom of the electrodes. This suggests that the location of the parallel devices or the direction of the injected flow has a major impact on the local flow field, and the ER cell with injection devices installed under the bottom of the electrodes has the advantage of obtaining a more turbulent flow field between electrodes.

4 Conclusions

1) The electrolyte flow field during the process of copper electro-refining was investigated with the aid of three-dimensional computational fluid dynamics simulation. Four computational models of ER cell with different setups of electrolyte inlets were established to examine and evaluate the characteristics of fluid flow and its uniformity in the inter-electrode spaces.

2) The VWAV values for the entire ER cell in both arrangements of CBI and TII are twice as large as that of SI. Specifically, the VWAV in the arrangement of BII is four times larger than that of SI. Such phenomena indicate that the velocity of electrolyte between electrodes can be improved when multiple injection devices are installed in the ER cell.

3) The application of parallel injection devices between electrodes helps to minimize the standard deviation and the relative range of the flow velocity. However, special attention should be paid to the arrangement of CBI. The relative range of the flow velocity in this case exceeds that of TII and BII more than 4 times due to its unequally spaced electrolyte inlets.

4) The turbulence intensity shows the same patterns as the VWAV, and it is almost twice as large as that of SI in the ER cell with the arrangement of BII, reflecting the fact that the parallel injection devices have the potential of generating turbulence and strengthening mass transfer of copper ions.

5) In general, one of the promising ways to supply fresh electrolyte rapidly and uniformly into the inter-electrode space is to adapt the ER cell with the arrangement of BII, i.e., to install parallel injection devices under the bottom of electrodes. By utilizing such an arrangement, the electro-refining under high electrical current density is possible, and the productivity can be increased in sequence.

References

[1] XUAN Shan-lun. Production practice for copper electrolysis under high current density [J]. China Nonferrous Metallurgy, 2007, 12(6): 27−28, 53. (in Chinese)

[2] LEAHY M J, SCHWARZ M P. Modeling natural convection in copper electrorefining: Describing turbulence behavior for industrial-sized systems [J]. Metallurgical and Materials Transactions B, 2011, 42(4): 875−890.

[3] IBL N, MÜLLER R H. Studies of natural convection at vertical electrodes [J]. Journal of the Electrochemical Society, 1958, 105(6): 346−353.

[4] VEILLEUX B, LAFRONT A M, GHALI E. Computerized scaled cells to study the effect of additive ratios and concentrations on nodulation during copper electrorefining [J]. Journal of Applied Electrochemistry, 2001, 31(9): 1017−1024.

[5] LIN Jian-xin, LI Xue-liang, CHEN Han-he, HE Jian-bo, WU Ji-lie. Cause of formation of nodular copper particles on electrorefined copper substrate [J]. Transactions of Nonferrous Metals Society of China, 1994, 4(4): 52−55.

[6] DENPO K, TERUTA S, FUKUNAKA Y, KONDO Y. Turbulent natural convection along a vertical electrode [J]. Metallurgical Transactions B, 1983, 14(4): 633−643.

[7] WENZL C, FILZWIESER A, KONETSCHNIK S. METTOP-BRX-technology-industrial application [C]//Proceeding of Chen Honorary Symposium on Hydrometallurgy, Electrometallurgy and Materials Characterization. New York: John Wiley & Sons, 2012: 61−75.

[8] KAWAI S, MIYAZAWA T. CFD modelling and simulation of industrial-scale copper electrorefining process [J]. Minerals Engineering, 2014, 63(4): 81−90.

[9] LEAHY M J, SCHWARZ M P. Experimental validation of a computational fluid dynamics model of copper electrowining [J]. Metallurgy and Materials Transactions B, 2010, 41(6): 1247−1260.

[10] YANG X G, ECKERT K, HEINZE A, UHLEMANN M. The concentration field during transient natural convection between vertical electrodes in a small-aspect-ratio cell [J]. Journal of Electroanalytical Chemistry, 2008, 613(1): 97−107.

[11] KAWAI S, NISHIKAWA K, FUKUNAKA Y, KIDA S. Numerical simulation of transient natural convection induced by electrochemical reactions confined between vertical plane Cu electrodes [J]. Electrochimica Acta, 2007, 53(1): 257−264.

[12] NELISSEN G, BOSSCHE B V D, DECONINCK J, THEEMSCHE A V, DAN C. Laminar and turbulent mass transfer simulations in a parallel plate reactor [J]. Journal of Applied Electrochemistry, 2003, 33(10): 863−873.

[13] LI Hao-lan, HU Jie, ZHOU Ping, WEI Wen-wu, SU Yin-biao. The optimization of operating conditions and structure parameters based on numerical simulation for electrolyte flow [J]. Transactions of Nonferrous Metals Society of China, 2014, 24(5): 1604−1609.

[14] MENTER F R. Two-equation eddy-viscosity turbulence models for engineering applications [J]. AIAA Journal, 2012, 32(8): 1598−1605.

[15] LIU H, LI P W, LEW J V. CFD study on flow distribution uniformity in fuel distributors having multiple structural bifurcation of flow channels [J]. International Journal of Hydrogen Energy, 2010, 35(17): 9186−9198.

[16] NELISSEN G, THEEMSCHE A V, DAN C, BOSSCHE B V D, DECONINCK J. Multi-ion transport and reaction simulations in turbulent parallel plate flow [J]. Journal of Electroanalytical Chemistry, 2004, 563(2): 213−220.

[17] HEMMATI H, MOHEBBI A, SOLTANI A, DANESHPAJOUH S. CFD modeling of the electrolyte flow in the copper electrorefining cell of Sarcheshmeh copper complex [J]. Hydrometallurgy, 2013, 139(3): 54−63.

不同进液方式下铜电解槽内电解液流动特性的评价

周 萍[1]，马海博[1]，谢紫微[1]，闫红杰[1]，Chenn Q. ZHOU[1,2]

1. 中南大学 能源科学与工程学院，长沙 410083；

2. Center for Innovation through Visualization and Simulation,
Purdue University Northwest, 2200 169th Street, Hammond, IN 46323, USA

摘 要：铜电解槽的进液口布置方式对极板间的流场有着显著的影响，而流场的分布决定电解过程中的电流分布。为了深入了解电解液在竖直极板间复杂的流动行为，以铜电解槽为研究对象，建立了针对“一端进液”、“底部中心进液”、“上侧交错进液”和“底部交错进液”4 种不同进液方式下电解槽内电解液的流动过程的三维计算流体动力学模型并进行数值模拟。结果表明：由于“底部中心进液”式电解槽中进液口的位置分布不均匀，其速度的极差较大，是交错进液时的 4 倍以上。另外，由于“底部交错进液”式电解槽内电解液的湍流强度较大, 因此其体平均速度是“一端进液”式的 4 倍。综合来看，“底部交错进液”式电解槽能够将新鲜的电解液快速、均匀地补充到极板间，为提高电流密度和增加产能奠定了基础。

关键词：铜电解精炼；进液口布置方式；流场均匀性；计算流体力学

(Edited by Wei-ping CHEN)